Supplement of

Long-term behavior and stability of calibration models for NO and NO₂ low cost sensors

Horim Kim[1], Michael Müller[1,2], Stephan Henne[1], and Christoph Hüglin[1]

[1]Laboratory for Air Pollution and Environmental Technology, Empa, 8600 Dübendorf, Switzerland
[2]now at: Amt für Geoinformation, Kanton Basel-Landschaft, 4410 Liestal, Switzerland.

Correspondence: Christoph Hüglin (christoph.hueglin@empa.ch)

S-1 Site description

S-1.1 Harkingen Monitoring station
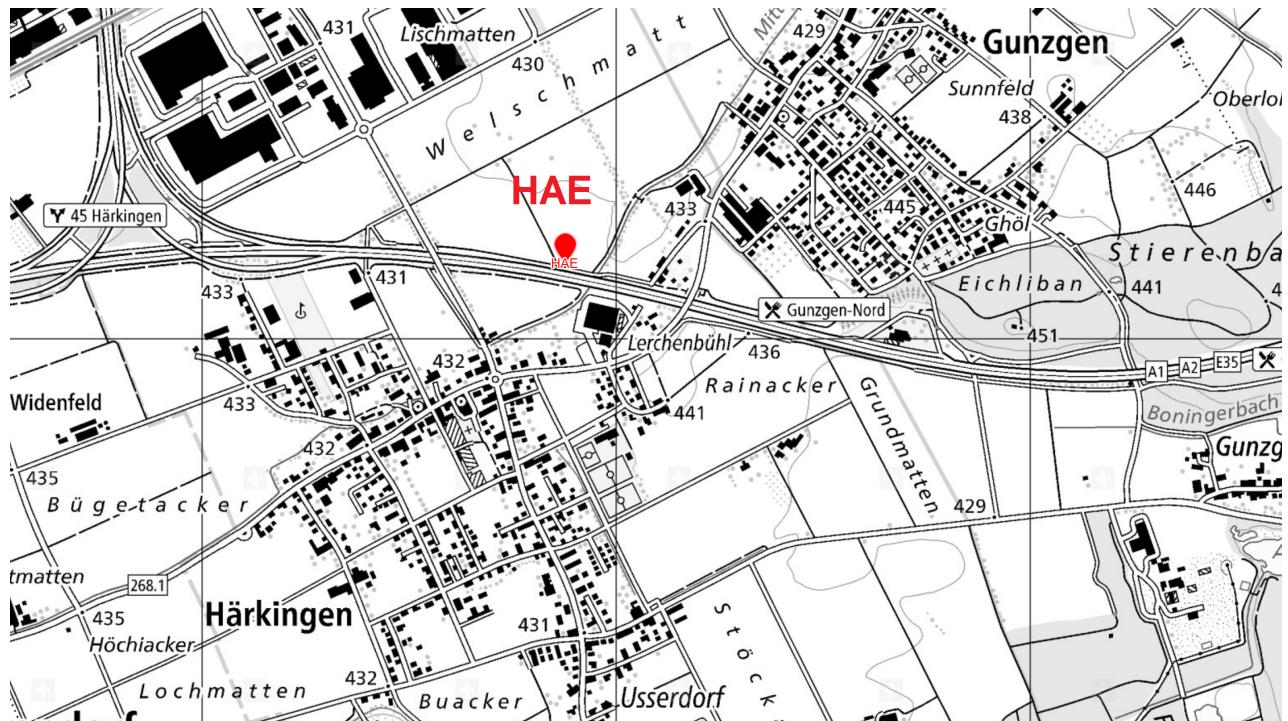
Figure S1. Geographical location of the reference monitoring site, Haerkingen air quality monitoring station. The map is obtained from the geo-mapping platform of the Swiss Confederation. © Swisstopo

| (a) View to the south-west side | (b) View to the north-east side |

Figure S2. Street view of Haerkingen air quality monitoring station. The images are provided by Empa.

S-1.2 Deployment sites
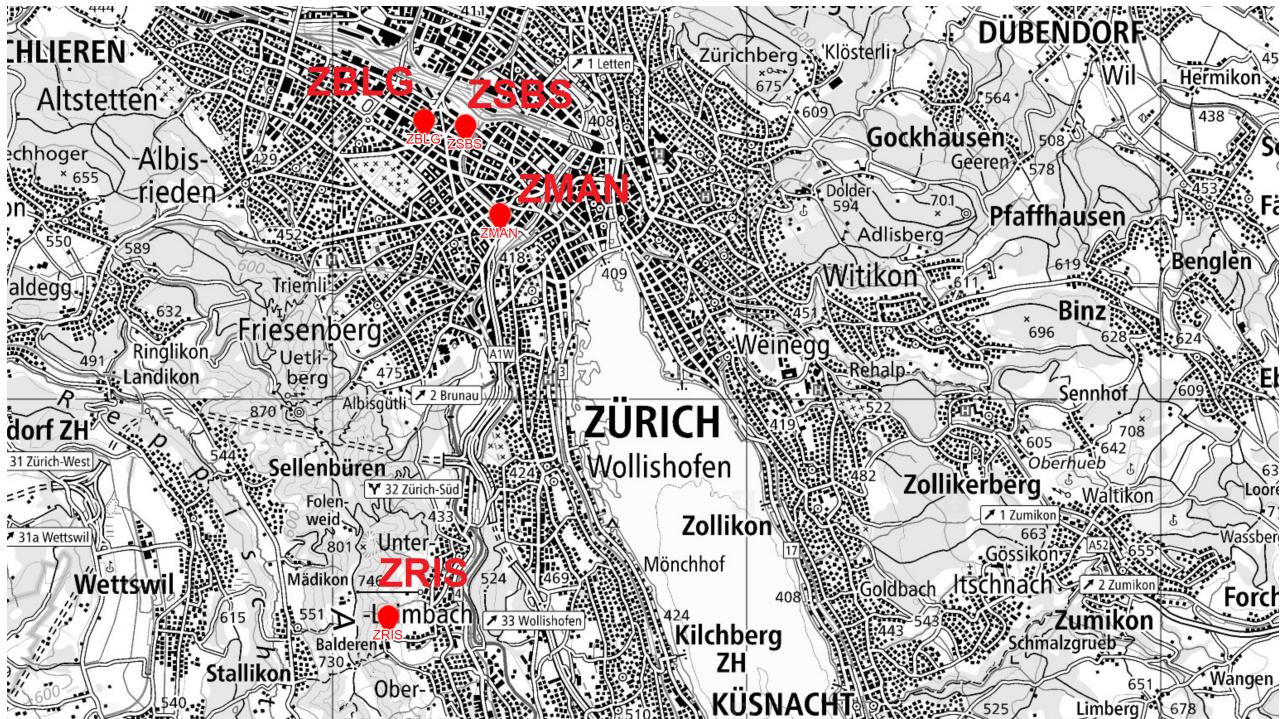
Figure S3. Geographical location of sensor units deployment sites in Zurich. The map is obtained from the geo-mapping platform of the Swiss Confederation. © Swisstopo

(a) ZRIS (AC009) (b) ZSBS (AC011)

(c) ZBLG (AC010) (d) ZMAN (AC012)

Figure S4. Street views of four sensor deployment sites in Zurich. All images of ZRIS, ZBLG, ZSBS, and ZMAN are provided by Empa.

S-2 Calibration model selection

5 ### S-2.1 Model variables

Table S1. List of variables for calibration models using robust linear regression. V_{sensor} indicates the raw signals from four sensor data (two NO sensors and two NO_2 sensors). T and RH parameter represents the temperature and relative humidity information respectively. D_{RH} parameter is presented in Section 2.3.

Model number	Model variables
RLM_1	offset(V_{sensor})
RLM_2	V_{sensor}
RLM_3	V_{sensor}, T
RLM_4	V_{sensor}, RH
RLM_5	V_{sensor}, T, RH
RLM_6	V_{sensor}, T, D_{RH_60}
RLM_7	V_{sensor}, T, D_{RH_90}
RLM_8	V_{sensor}, T, D_{RH_120}
RLM_9	V_{sensor}, T, D_{RH_150}
RLM_10	V_{sensor}, RH, D_{RH_60}
RLM_11	V_{sensor}, RH, D_{RH_90}
RLM_12	V_{sensor}, RH, D_{RH_120}
RLM_13	V_{sensor}, RH, D_{RH_150}
RLM_14	V_{sensor}, T, RH, D_{RH_60}
RLM_15	V_{sensor}, T, RH, D_{RH_90}
RLM_16	V_{sensor}, T, RH, D_{RH_120}
RLM_17	V_{sensor}, T, RH, D_{RH_150}
RLM_18	V_{sensor}, T, V_{sensor}*T
RLM_19	V_{sensor}, T, V_{sensor}*T, D_{RH_60}
RLM_20	V_{sensor}, T, V_{sensor}*T, D_{RH_90}
RLM_21	V_{sensor}, T, V_{sensor}*T, D_{RH_120}
RLM_22	V_{sensor}, T, V_{sensor}*T, D_{RH_150}

Table S2. List of variables for calibration models using random forest regression. V_{sensor} indicates the raw signals from four sensor data (two NO sensors and two NO_2 sensors). T and RH parameter represents the temperature and relative humidity information respectively. D_{RH} parameter is presented in Section 2.3.

Model number	Model variables
RF_1	V_{sensor}
RF_2	V_{sensor}, T
RF_3	V_{sensor}, T, D_{RH_60}
RF_4	V_{sensor}, T, D_{RH_90}
RF_5	V_{sensor}, T, D_{RH_120}
RF_6	V_{sensor}, T, D_{RH_150}
RF_7	V_{sensor}, RH
RF_8	V_{sensor}, T, RH
RF_9	V_{sensor}, T, $V_{sensor}*T$

S-2.2   Results for the statistical metrics

Table S3. nRMSE values of all calibration models for NO and NO_2 sensors during the model selection process.

Model	AC009				AC010				AC011				AC012			
	NO		NO_2		NO		NO_2		NO		NO_2		NO		NO_2	
	A	B	A	B	A	B	A	B	A	B	A	B	A	B	A	B
RLM_1	0.658	0.673	0.800	0.785	0.704	0.737	0.785	0.765	0.715	0.694	0.882	0.785	0.779	0.729	0.832	0.784
RLM_2	0.507	0.569	0.760	0.653	0.590	0.666	0.749	0.625	0.617	0.591	0.885	0.724	0.702	0.649	0.816	0.643
RLM_3	0.463	0.513	0.686	0.557	0.507	0.536	0.668	0.549	0.499	0.551	0.847	0.654	0.432	0.568	0.747	0.558
RLM_4	0.490	0.555	0.668	0.574	0.565	0.620	0.666	0.566	0.551	0.577	0.856	0.660	0.547	0.627	0.752	0.545
RLM_5	0.442	0.475	0.667	0.556	0.474	0.498	0.657	0.548	0.486	0.530	0.847	0.650	0.423	0.517	0.742	0.542
RLM_6	0.463	0.513	0.629	0.441	0.507	0.536	0.584	0.441	0.498	0.551	0.802	0.540	0.430	0.563	0.682	0.484
RLM_7	0.463	0.510	0.608	0.426	0.505	0.533	0.556	0.423	0.499	0.550	0.784	0.507	0.431	0.557	0.663	0.457
RLM_8	0.461	0.505	0.589	0.420	0.502	0.530	0.533	0.413	0.499	0.548	0.766	0.480	0.432	0.550	0.647	0.434
RLM_9	0.458	0.500	0.575	0.420	0.498	0.526	0.516	0.409	0.499	0.545	0.751	0.462	0.432	0.543	0.636	0.415
RLM_10	0.490	0.554	0.610	0.478	0.564	0.619	0.580	0.468	0.550	0.577	0.811	0.547	0.547	0.624	0.691	0.471
RLM_11	0.490	0.553	0.596	0.469	0.563	0.618	0.561	0.456	0.551	0.577	0.797	0.523	0.547	0.619	0.679	0.450
RLM_12	0.488	0.549	0.585	0.467	0.561	0.615	0.546	0.450	0.551	0.576	0.785	0.504	0.546	0.614	0.672	0.434
RLM_13	0.486	0.546	0.576	0.468	0.558	0.612	0.536	0.448	0.550	0.574	0.775	0.491	0.545	0.608	0.666	0.422
RLM_14	0.442	0.475	0.609	0.441	0.473	0.498	0.567	0.440	0.482	0.529	0.799	0.532	0.416	0.516	0.675	0.465
RLM_15	0.442	0.475	0.594	0.425	0.474	0.498	0.544	0.423	0.484	0.530	0.782	0.503	0.418	0.514	0.659	0.442
RLM_16	0.442	0.474	0.581	0.417	0.473	0.498	0.525	0.412	0.485	0.530	0.766	0.479	0.420	0.511	0.646	0.424
RLM_17	0.442	0.472	0.569	0.414	0.472	0.497	0.511	0.407	0.486	0.529	0.751	0.462	0.421	0.508	0.636	0.409
RLM_18	0.270	0.306	0.586	0.497	0.312	0.343	0.609	0.522	0.315	0.324	0.773	0.608	0.294	0.360	0.650	0.519
RLM_19	0.268	0.302	0.507	0.368	0.307	0.336	0.503	0.409	0.314	0.320	0.666	0.471	0.293	0.343	0.519	0.440
RLM_20	0.267	0.298	0.479	0.356	0.303	0.330	0.471	0.392	0.312	0.318	0.628	0.434	0.291	0.335	0.484	0.412
RLM_21	0.265	0.294	0.454	0.354	0.299	0.325	0.446	0.384	0.310	0.314	0.594	0.406	0.289	0.328	0.458	0.388
RLM_22	0.263	0.290	0.436	0.358	0.295	0.320	0.429	0.382	0.308	0.311	0.566	0.387	0.286	0.321	0.440	0.370
RLM_23	0.268	0.302	0.507	0.368	0.307	0.336	0.503	0.409	0.314	0.320	0.666	0.471	0.293	0.343	0.519	0.440
RLM_24	0.267	0.298	0.479	0.356	0.303	0.330	0.471	0.392	0.312	0.318	0.628	0.434	0.291	0.335	0.484	0.412
RLM_25	0.265	0.294	0.454	0.354	0.299	0.325	0.446	0.384	0.310	0.314	0.594	0.406	0.289	0.328	0.458	0.388
RLM_26	0.263	0.290	0.436	0.358	0.295	0.320	0.429	0.382	0.308	0.311	0.566	0.387	0.286	0.321	0.440	0.370
RF_1	0.425	0.490	0.626	0.566	0.532	0.616	0.663	0.562	0.561	0.500	0.784	0.645	0.664	0.569	0.687	0.580
RF_2	0.228	0.254	0.519	0.472	0.259	0.277	0.557	0.469	0.255	0.267	0.726	0.569	0.242	0.296	0.596	0.461
RF_3	0.236	0.257	0.372	0.297	0.260	0.274	0.405	0.311	0.252	0.261	0.584	0.368	0.247	0.283	0.400	0.329
RF_4	0.232	0.253	0.349	0.292	0.257	0.270	0.383	0.300	0.252	0.261	0.551	0.344	0.244	0.278	0.375	0.312
RF_5	0.231	0.252	0.335	0.294	0.257	0.269	0.365	0.295	0.253	0.260	0.521	0.331	0.243	0.274	0.363	0.302
RF_6	0.229	0.250	0.326	0.299	0.257	0.268	0.354	0.295	0.251	0.258	0.503	0.322	0.241	0.273	0.354	0.295
RF_7	0.314	0.363	0.521	0.492	0.426	0.476	0.581	0.503	0.380	0.388	0.735	0.589	0.395	0.454	0.623	0.479
RF_8	0.229	0.248	0.486	0.461	0.247	0.259	0.532	0.458	0.248	0.257	0.688	0.548	0.242	0.278	0.565	0.441
RF_9	0.229	0.254	0.519	0.472	0.259	0.277	0.557	0.469	0.255	0.267	0.726	0.568	0.241	0.295	0.596	0.461

Table S4. R^2 values of all calibration models for NO and NO$_2$ sensors during the model selection process.

| | AC009 | | | | AC010 | | | | AC011 | | | | AC012 | | | |
| | NO | | NO$_2$ | | NO | | NO$_2$ | | NO | | NO$_2$ | | NO | | NO$_2$ | |
Model	A	B	A	B	A	B	A	B	A	B	A	B	A	B	A	B
RLM_ 1	0.744	0.677	0.435	0.587	0.652	0.559	0.448	0.615	0.620	0.651	0.227	0.483	0.509	0.582	0.341	0.590
RLM_ 2	0.744	0.677	0.435	0.587	0.652	0.559	0.448	0.615	0.620	0.651	0.227	0.483	0.509	0.582	0.341	0.590
RLM_ 3	0.793	0.738	0.532	0.691	0.749	0.716	0.555	0.699	0.764	0.706	0.287	0.574	0.814	0.679	0.443	0.688
RLM_ 4	0.761	0.693	0.558	0.673	0.681	0.618	0.558	0.681	0.698	0.668	0.273	0.565	0.701	0.609	0.437	0.703
RLM_ 5	0.810	0.777	0.559	0.693	0.783	0.756	0.570	0.700	0.778	0.732	0.288	0.578	0.823	0.735	0.451	0.707
RLM_ 6	0.793	0.739	0.608	0.808	0.749	0.716	0.661	0.807	0.765	0.706	0.365	0.710	0.817	0.685	0.543	0.766
RLM_ 7	0.793	0.742	0.635	0.821	0.751	0.719	0.693	0.822	0.764	0.707	0.396	0.745	0.815	0.691	0.571	0.792
RLM_ 8	0.795	0.746	0.658	0.826	0.754	0.722	0.719	0.830	0.764	0.710	0.425	0.771	0.815	0.699	0.595	0.813
RLM_ 9	0.797	0.751	0.677	0.826	0.758	0.726	0.737	0.833	0.764	0.713	0.450	0.789	0.814	0.707	0.613	0.828
RLM_ 10	0.761	0.694	0.635	0.776	0.682	0.619	0.667	0.783	0.699	0.668	0.354	0.703	0.701	0.613	0.538	0.779
RLM_ 11	0.761	0.696	0.654	0.784	0.683	0.621	0.691	0.794	0.698	0.668	0.380	0.730	0.701	0.619	0.558	0.798
RLM_ 12	0.762	0.699	0.670	0.786	0.685	0.624	0.708	0.799	0.698	0.669	0.403	0.749	0.702	0.626	0.573	0.813
RLM_ 13	0.764	0.703	0.681	0.785	0.688	0.628	0.719	0.800	0.699	0.672	0.423	0.762	0.703	0.632	0.584	0.823
RLM_ 14	0.811	0.777	0.636	0.808	0.783	0.756	0.681	0.807	0.781	0.734	0.371	0.718	0.828	0.736	0.556	0.784
RLM_ 15	0.811	0.777	0.656	0.822	0.783	0.756	0.708	0.822	0.779	0.733	0.400	0.749	0.826	0.738	0.580	0.805
RLM_ 16	0.810	0.778	0.673	0.829	0.783	0.756	0.728	0.831	0.778	0.733	0.428	0.772	0.825	0.741	0.600	0.821
RLM_ 17	0.811	0.780	0.686	0.830	0.784	0.757	0.742	0.835	0.778	0.733	0.451	0.789	0.824	0.744	0.615	0.834
RLM_ 18	0.927	0.906	0.658	0.754	0.902	0.882	0.632	0.729	0.901	0.896	0.407	0.632	0.914	0.871	0.580	0.732
RLM_ 19	0.928	0.909	0.745	0.864	0.906	0.887	0.749	0.833	0.902	0.898	0.560	0.779	0.914	0.882	0.733	0.807
RLM_ 20	0.929	0.911	0.772	0.873	0.908	0.891	0.780	0.847	0.903	0.900	0.609	0.813	0.915	0.888	0.768	0.831
RLM_ 21	0.930	0.914	0.795	0.875	0.911	0.894	0.802	0.853	0.904	0.902	0.650	0.836	0.917	0.893	0.793	0.850
RLM_ 22	0.931	0.916	0.811	0.872	0.913	0.898	0.817	0.854	0.906	0.903	0.682	0.850	0.918	0.897	0.808	0.864
RLM_ 23	0.928	0.909	0.745	0.864	0.906	0.887	0.749	0.833	0.902	0.898	0.560	0.779	0.914	0.882	0.733	0.807
RLM_ 24	0.929	0.911	0.772	0.873	0.908	0.891	0.780	0.847	0.903	0.900	0.609	0.813	0.915	0.888	0.768	0.831
RLM_ 25	0.930	0.914	0.795	0.875	0.911	0.894	0.802	0.853	0.904	0.902	0.650	0.836	0.917	0.893	0.793	0.850
RLM_ 26	0.931	0.916	0.811	0.872	0.913	0.898	0.817	0.854	0.906	0.903	0.682	0.850	0.918	0.897	0.808	0.864
RF_ 1	0.820	0.760	0.608	0.680	0.717	0.622	0.561	0.685	0.686	0.750	0.387	0.585	0.559	0.677	0.529	0.663
RF_ 2	0.948	0.936	0.731	0.777	0.933	0.923	0.690	0.780	0.935	0.929	0.473	0.677	0.942	0.913	0.645	0.788
RF_ 3	0.949	0.939	0.867	0.917	0.934	0.928	0.843	0.909	0.939	0.934	0.666	0.872	0.944	0.924	0.849	0.898
RF_ 4	0.951	0.941	0.885	0.922	0.936	0.930	0.861	0.916	0.938	0.934	0.704	0.889	0.945	0.927	0.869	0.910
RF_ 5	0.950	0.941	0.896	0.920	0.936	0.930	0.875	0.919	0.938	0.934	0.737	0.898	0.946	0.929	0.879	0.916
RF_ 6	0.952	0.942	0.902	0.917	0.936	0.930	0.883	0.919	0.939	0.935	0.756	0.904	0.946	0.929	0.885	0.920
RF_ 7	0.902	0.868	0.728	0.758	0.819	0.773	0.662	0.747	0.856	0.850	0.460	0.653	0.844	0.794	0.612	0.771
RF_ 8	0.952	0.944	0.767	0.789	0.942	0.936	0.720	0.792	0.940	0.936	0.529	0.702	0.945	0.927	0.686	0.810
RF_ 9	0.948	0.937	0.731	0.777	0.933	0.923	0.690	0.780	0.935	0.929	0.473	0.677	0.942	0.913	0.645	0.788

S-3   Sensor performance

S-3.1   Calibration evaluation
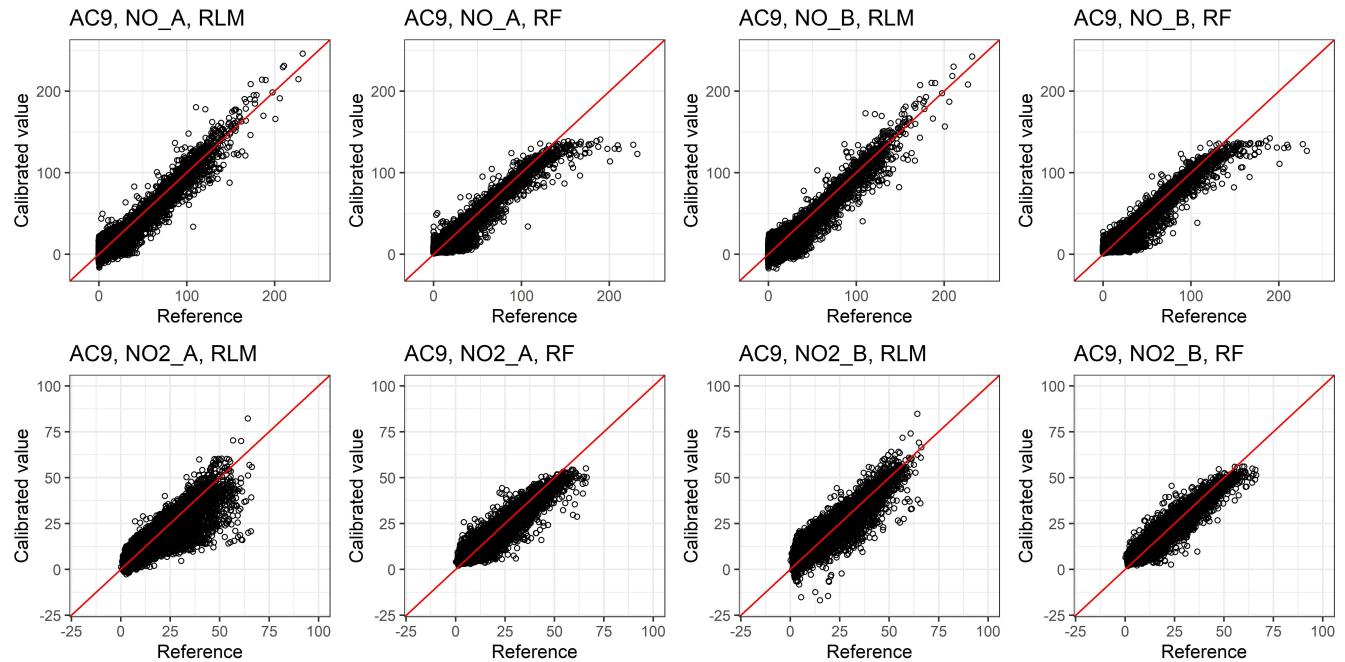
Figure S5. Calibrated and Reference concentrations in AC009 during the first co-location campaign. Red line in the plot indicates 1:1 identity line.
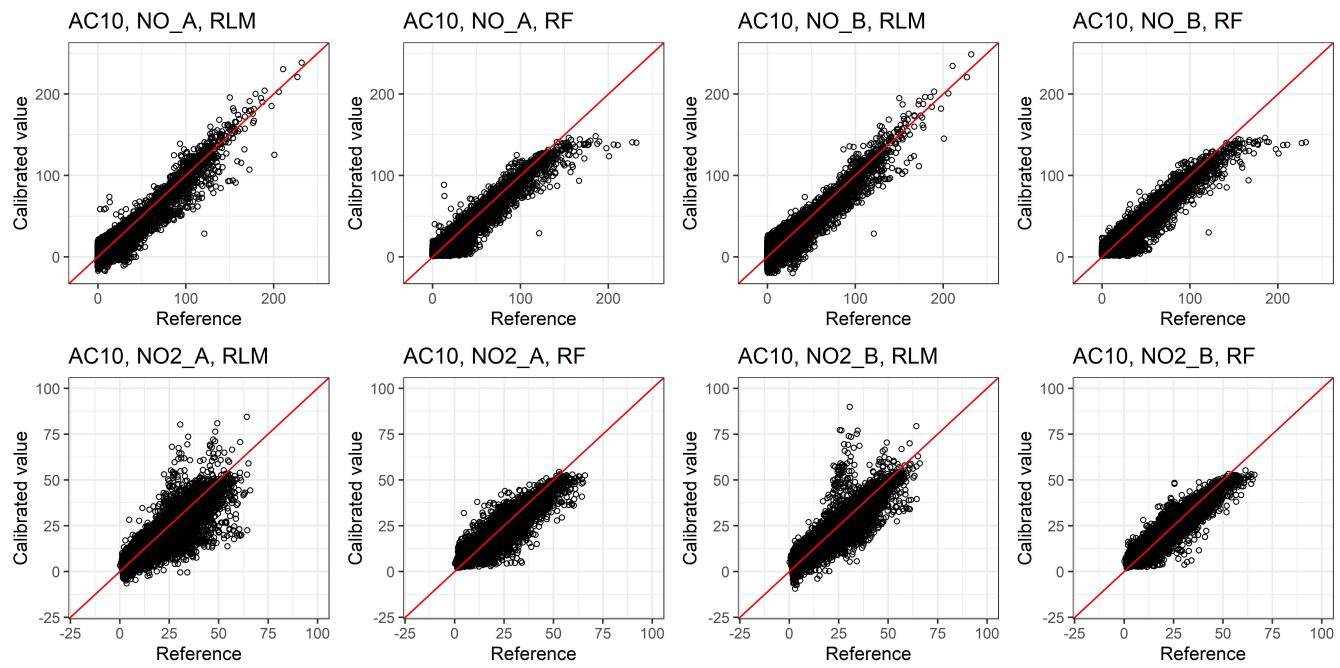
Figure S6. Calibrated and Reference concentrations in AC010 during the first co-location campaign. Red line in the plot indicates 1:1 identity line.
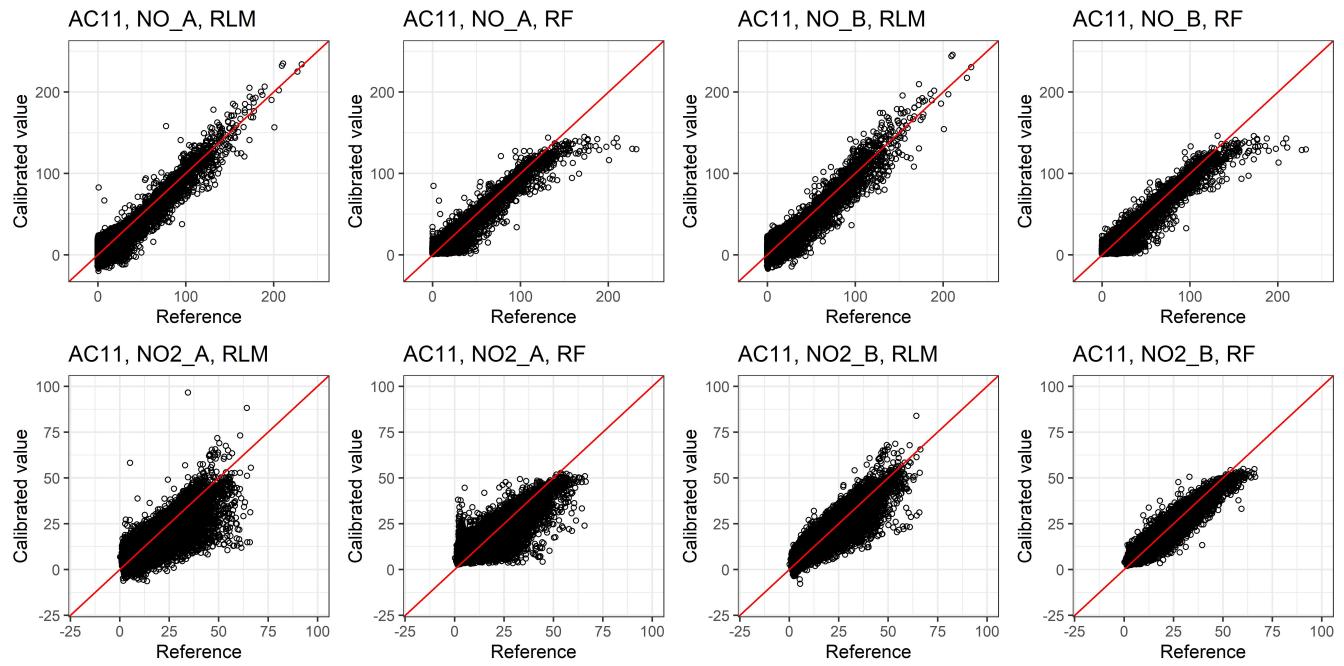
Figure S7. Calibrated and Reference concentrations in AC011 during the first co-location campaign. Red line in the plot indicates 1:1 identity line.
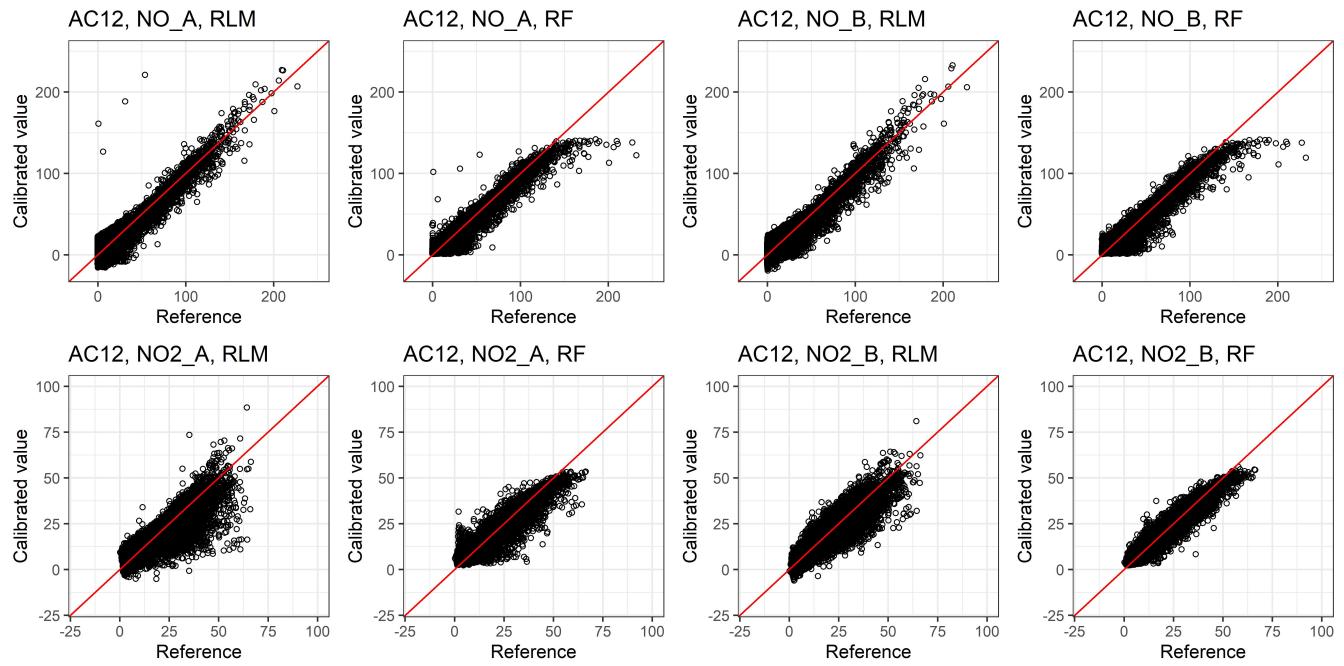
Figure S8. Calibrated and Reference concentrations in AC012 during the first co-location campaign. Red line in the plot indicates 1:1 identity line.

Table S5. Statistical metrics for all NO and NO_2 sensors during during the first and second co-location campaigns.

Unit	Sensor	RMSE [ppb]				MBE [ppb]				R^2 [-]				nRMSE [-]			
		RLM		RF		RLM		RF		RLM		RF		RLM		RF	
		1st	2nd	1st	2nd	1st	2nd	1st	2nd	1st	2nd	1st	2nd	1st	2nd	1st	2nd
AC009	NO_00	7.43	6.57	6.52	5.70	-0.20	-2.04	-0.03	-0.32	0.93	0.96	0.95	0.96	0.27	0.25	0.24	0.22
	NO_01	8.13	7.28	7.05	6.49	-0.24	-1.01	-0.03	0.74	0.91	0.95	0.94	0.94	0.29	0.28	0.26	0.25
	NO2_00	4.89	5.70	3.03	5.29	-0.51	1.89	-0.02	2.32	0.81	0.75	0.93	0.80	0.44	0.55	0.27	0.51
	NO2_01	3.96	7.07	2.83	6.62	0.00	2.86	-0.02	2.88	0.87	0.63	0.94	0.68	0.35	0.68	0.25	0.63
AC010	NO_00	7.65	10.14	6.67	8.40	-0.30	-7.66	-0.03	-2.85	0.92	0.96	0.94	0.92	0.29	0.39	0.25	0.32
	NO_01	8.32	7.28	7.05	6.79	-0.23	-0.72	-0.03	0.29	0.90	0.95	0.93	0.93	0.31	0.28	0.27	0.26
	NO2_00	4.95	6.73	3.45	6.33	-0.34	3.07	-0.02	3.19	0.81	0.66	0.91	0.74	0.44	0.66	0.30	0.62
	NO2_01	4.40	6.38	2.90	5.85	-0.07	1.77	-0.01	2.50	0.85	0.64	0.94	0.77	0.39	0.62	0.26	0.57
AC011	NO_00	7.77	7.28	6.63	5.81	-0.21	1.10	-0.03	1.61	0.91	0.96	0.94	0.95	0.29	0.28	0.25	0.22
	NO_01	7.94	7.97	6.84	6.34	-0.22	1.00	-0.03	1.44	0.91	0.95	0.94	0.94	0.30	0.30	0.26	0.24
	NO2_00	6.41	8.44	5.21	7.91	-0.60	3.52	-0.01	3.69	0.69	0.50	0.79	0.55	0.56	0.81	0.46	0.76
	NO2_01	4.35	7.33	3.03	6.96	-0.21	2.98	-0.02	2.84	0.85	0.60	0.93	0.63	0.38	0.71	0.27	0.67
AC012	NO_00	7.79	6.64	6.64	5.95	-0.20	1.28	-0.03	1.85	0.92	0.96	0.94	0.95	0.29	0.26	0.25	0.23
	NO_01	8.30	7.72	7.27	6.28	-0.21	-0.41	-0.03	1.30	0.90	0.95	0.93	0.94	0.31	0.30	0.27	0.25
	NO2_00	5.08	6.70	3.44	5.36	-0.52	-1.35	-0.03	-0.18	0.80	0.66	0.91	0.73	0.44	0.65	0.30	0.52
	NO2_01	4.26	5.90	2.85	5.03	-0.20	1.02	-0.02	1.45	0.86	0.71	0.94	0.78	0.37	0.58	0.25	0.49
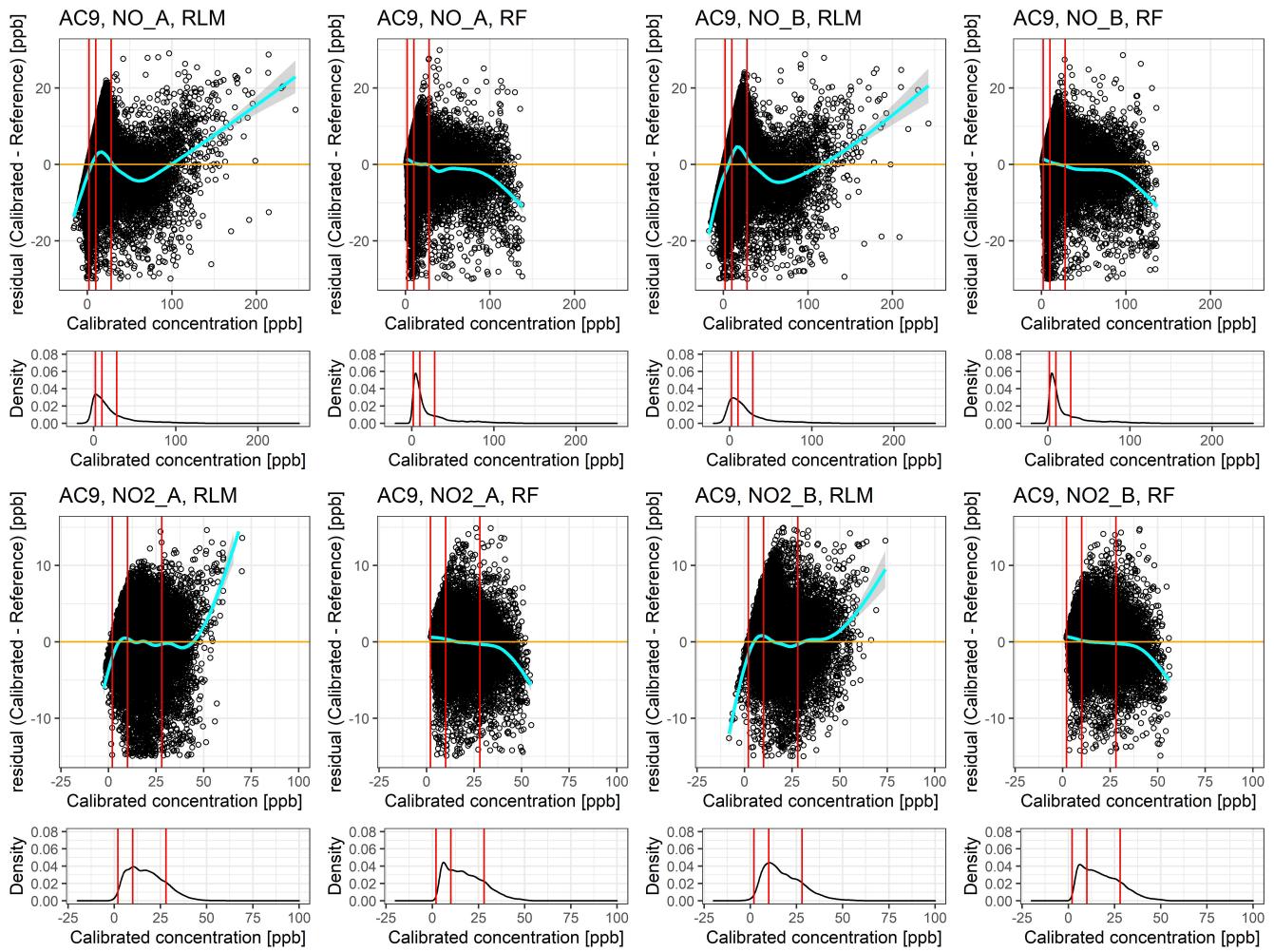
Figure S9. Residual plots for the predicted concentrations of AC009 at the first co-location campaign. A distribution density of predicted concentration was illustrated below each residual plots. Vertical red lines in the plots indicate 25%, 50%, and 75% quantile of the reference concentration. A horizontal orange line indicates x-axis (0 ppb of residual). Moreover, smoothed means of residual at each calibrated values are presented as cyan-colored curves.
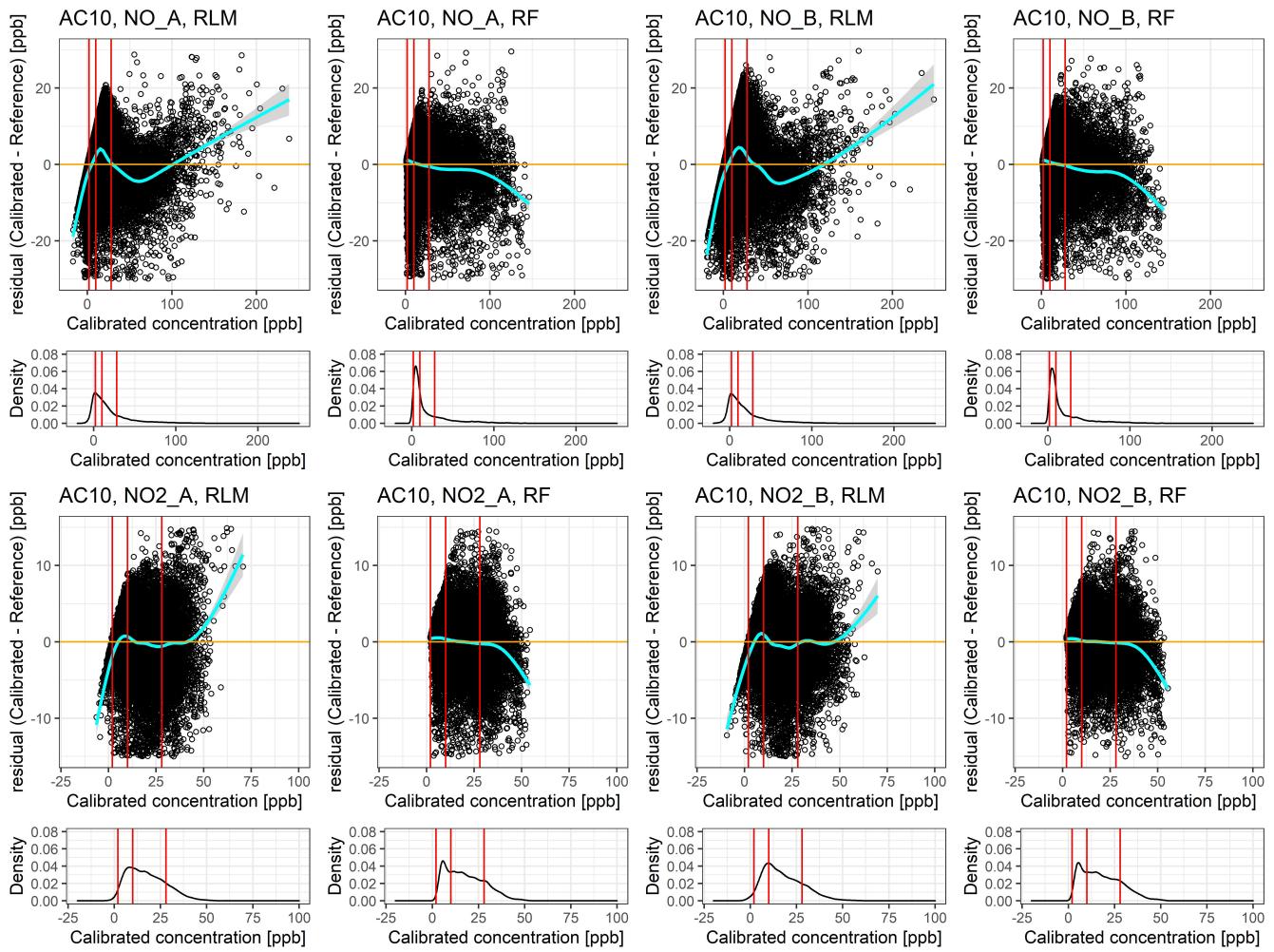
Figure S10. Residual plots for the predicted concentrations of AC010 at the first co-location campaign. A distribution density of predicted concentration was illustrated below each residual plots. Vertical red lines in the plots indicate 25%, 50%, and 75% quantile of the reference concentration. A horizontal orange line indicates x-axis (0 ppb of residual). Moreover, smoothed means of residual at each calibrated values are presented as cyan-colored curves.
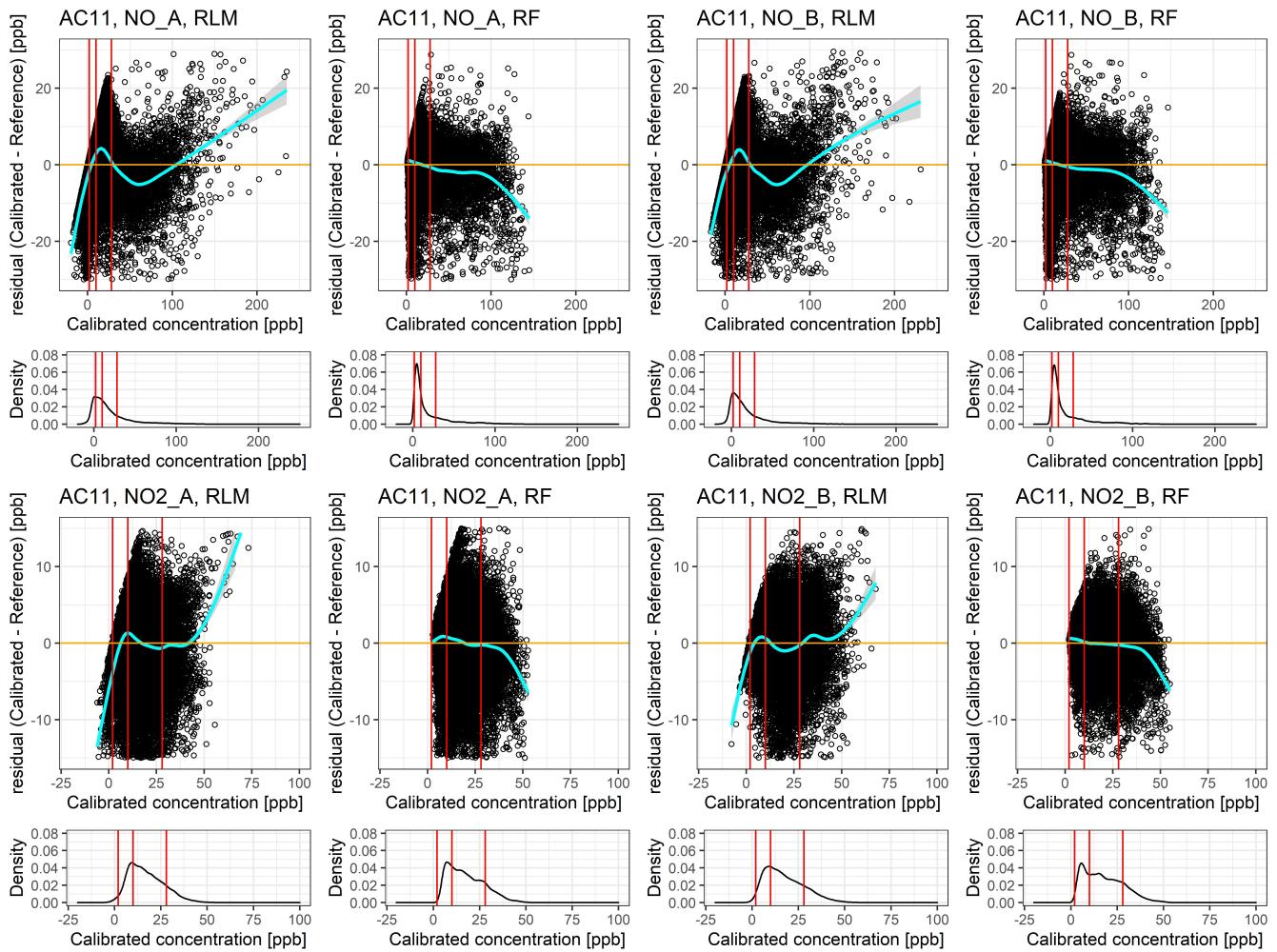
Figure S11. Residual plots for the predicted concentrations of AC011 at the first co-location campaign. A distribution density of predicted concentration was illustrated below each residual plots. Vertical red lines in the plots indicate 25%, 50%, and 75% quantile of the reference concentration. A horizontal orange line indicates x-axis (0 ppb of residual). Moreover, smoothed means of residual at each calibrated values are presented as cyan-colored curves.
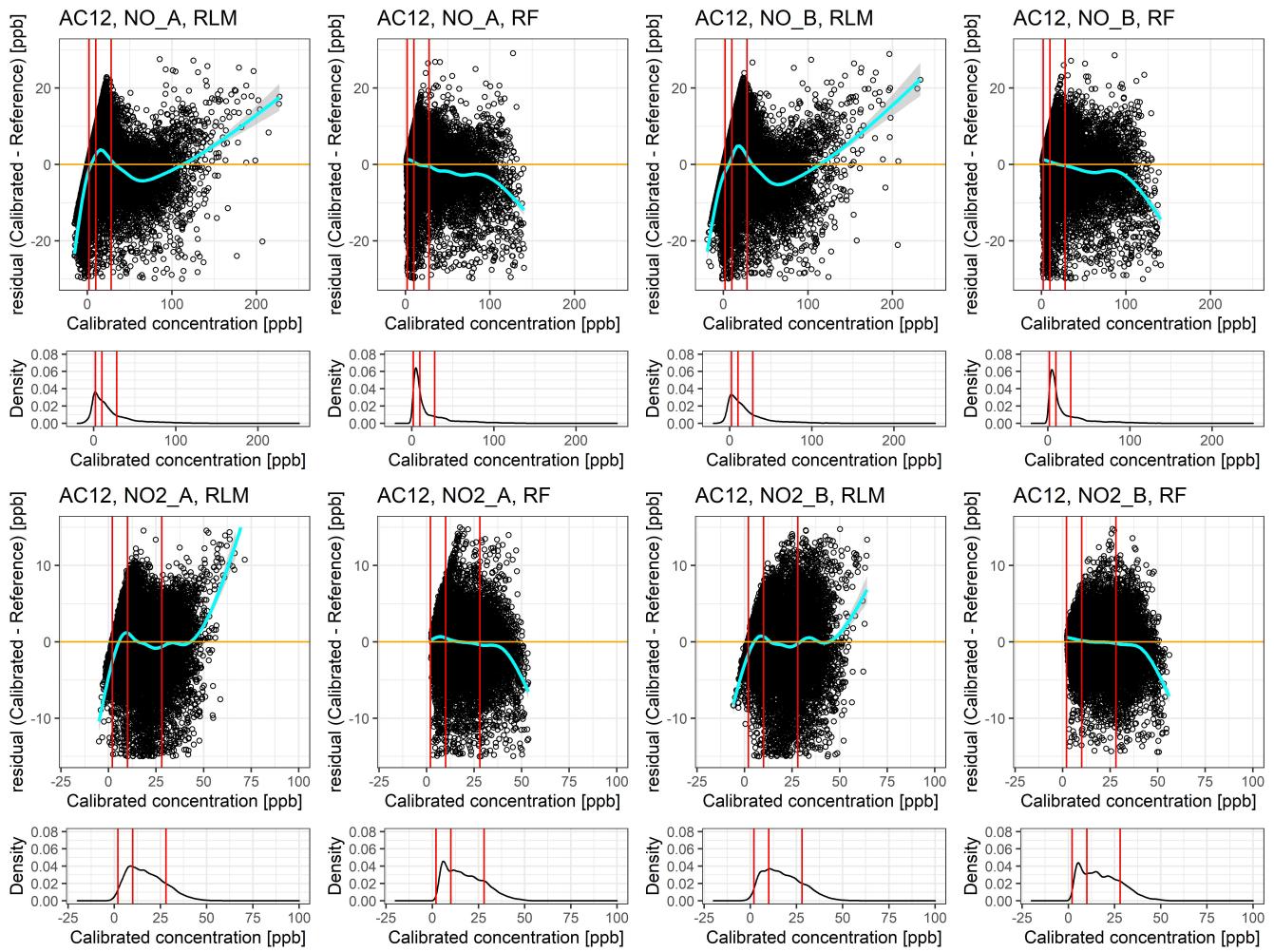
Figure S12. Residual plots for the predicted concentrations of AC012 at the first co-location campaign. A distribution density of predicted concentration was illustrated below each residual plots. Vertical red lines in the plots indicate 25%, 50%, and 75% quantile of the reference concentration. A horizontal orange line indicates x-axis (0 ppb of residual). Moreover, smoothed means of residual at each calibrated values are presented as cyan-colored curves.

S-3.2 Deployment periods
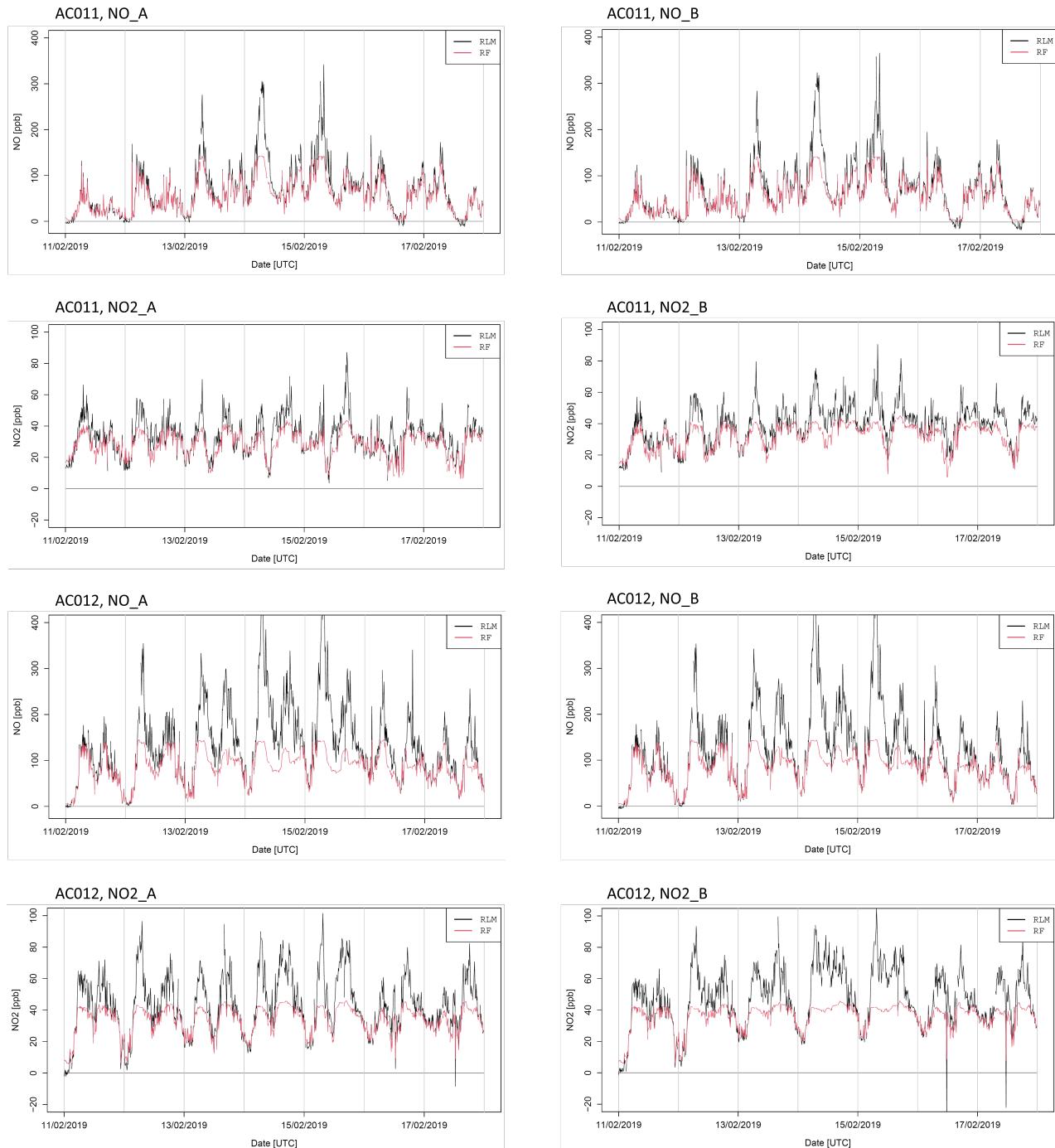
Figure S13. Examples of the time-series of AC011 and AC012 during the deployment period. The time-series visualize the upper limitation of the prediction by the random forest regression.
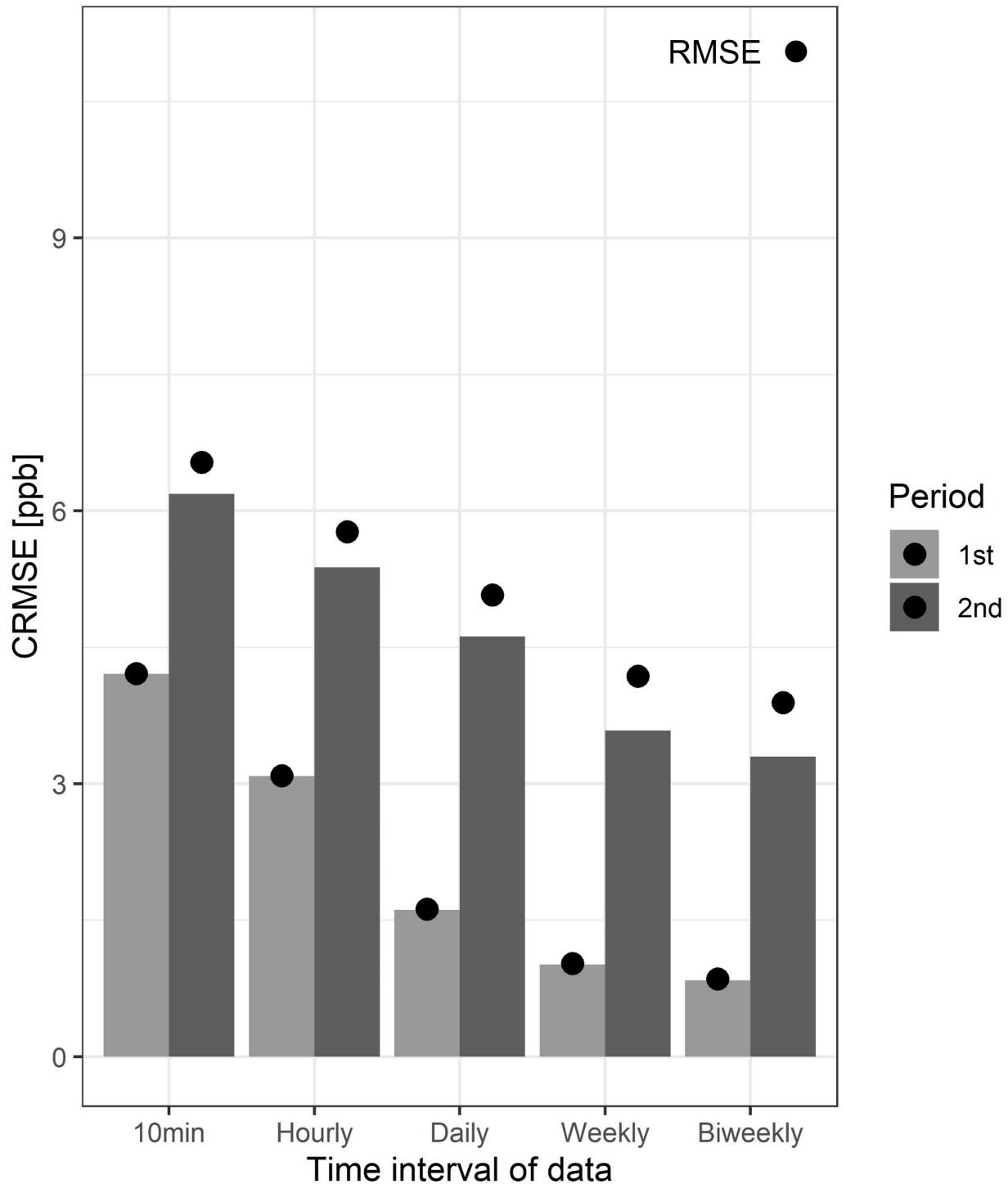
Figure S14. Statistical metrics of NO_2 sensors depending on the time interval. Figure demonstrates that RMSE and CRMSE values in two periods of co-location site decreases as the time interval increases from 10-minutes to bi-weekly resolution.

10   S-3.3   Assessment of sensor performance after deployment

S-3.3.1   Data filtering

To identify malfunctioning sensors, following steps were implemented in all sensor units: For the first step, the malfunctioning period was pre-selected from the NO_A sensor of each unit. Two time-series were mainly observed for the detection. (1) I detected the malfunction period from the time-series contained sensor raw-signal data (S_{raw}) and reference concentration
15 (S_{ref}). (2) With the time-series of $|\Delta S_{raw}|$ and $|\Delta S_{ref}|$, I checked again the discrepancy between the dynamics of two data. For the second step, I checked whether the pre-selection periods from the NO_A sensor were in accordance with those from NO_B, NO2_A, NO2_B sensors. As a result, only the periods detected concurrently in all four sensors were filtered. This is because the malfunctioning was possibly caused by the external environmental factors outside of the sensor unit and would affect simultaneously to every sensors.

Sensor	Start	End
AC009	2020-01-28 8:00	2020-01-28 14:00
	2020-02-04 3:00	2020-02-05 4:00
	2020-02-10 4:00	2020-02-10 11:00
	2020-02-13 17:00	2020-02-14 13:00
	2020-03-10 14:00	2020-03-11 12:00
AC010	2020-01-28 8:00	2020-01-28 14:00
	2020-02-04 2:00	2020-02-04 13:00
	2020-02-10 4:00	2020-02-10 13:00
	2020-02-11 4:00	2020-02-11 13:00
	2020-02-13 17:00	2020-02-14 11:00
	2020-02-18 00:00	2020-02-18 13:00
	2020-02-19 9:00	2020-02-19 19:00
	2020-02-25 14:00	2020-02-27 21:00
	2020-02-29 17:00	2020-03-03 11:00
	2020-03-06 4:00	2020-03-06 11:00
	2020-03-10 9:00	2020-03-11 12:00
AC011	2019-12-22 17:00	2019-12-23 16:00
	2020-01-28 8:00	2020-01-28 13:00
	2020-02-04 3:00	2020-02-04 19:00
	2020-02-11 4:00	2020-02-11 13:00
	2020-02-13 17:00	2020-02-14 8:00
	2020-02-26 3:00	2020-02-26 10:00
	2020-02-29 16:00	2020-03-01 12:00
	2020-03-01 18:00	2020-03-02 17:00
	2020-03-10 11:00	2020-03-11 14:00
AC012	2020-01-28 8:00	2020-01-28 13:00
	2020-02-13 17:00	2020-02-14 14:00
	2020-03-10 13:00	2020-03-11 12:00

Table S6. Data filtering periods. The data obtained in the periods shown in the table are filtered for the performance analysis in the co-location period after deployment (second co-location campaign). The filtering method is based on the sensor malfunctioning, which was detected by observing the time-series of sensor raw-signal and reference pollutant concentration.
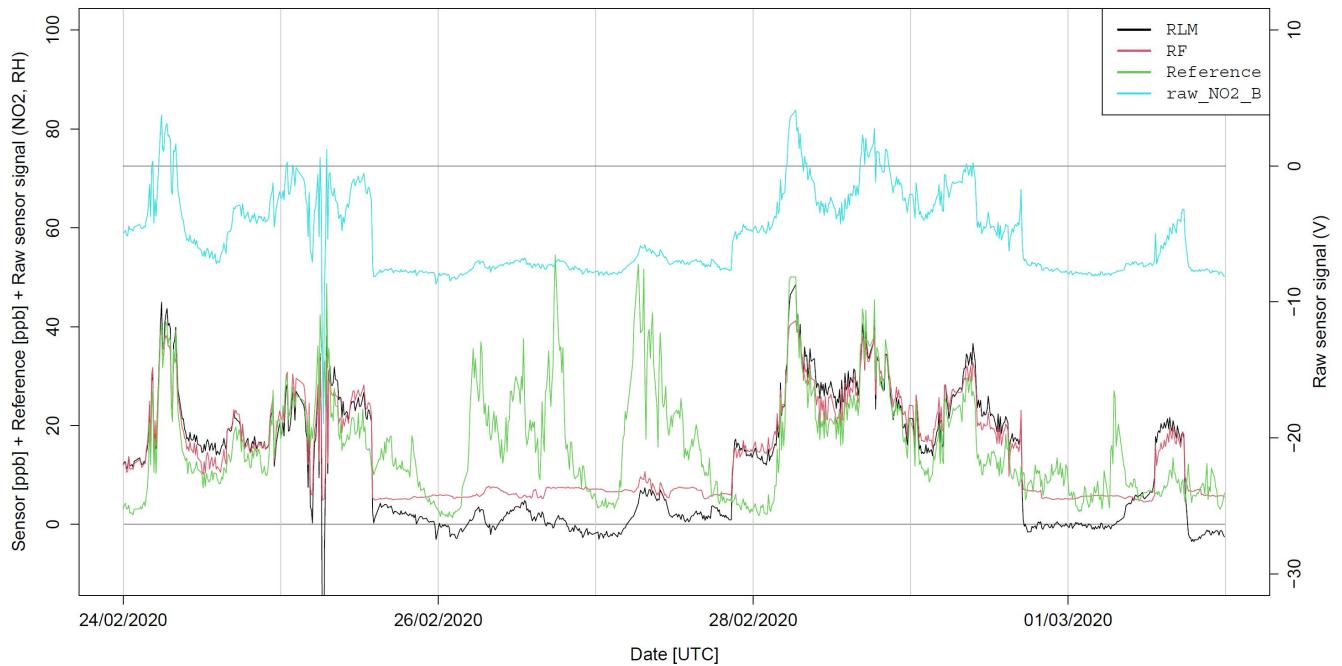
Figure S15. An example of sensor malfunctioning period from the NO2_B sensor of AC010. From 2020-02-25 to 2020-02-28, raw signals of the sensor (raw_NO2_B) during the period did not show any dynamics as the reference data, thus the severe under-estimation is obtained in the model prediction.

20   **S-3.3.2   Senor performance after the deployment**
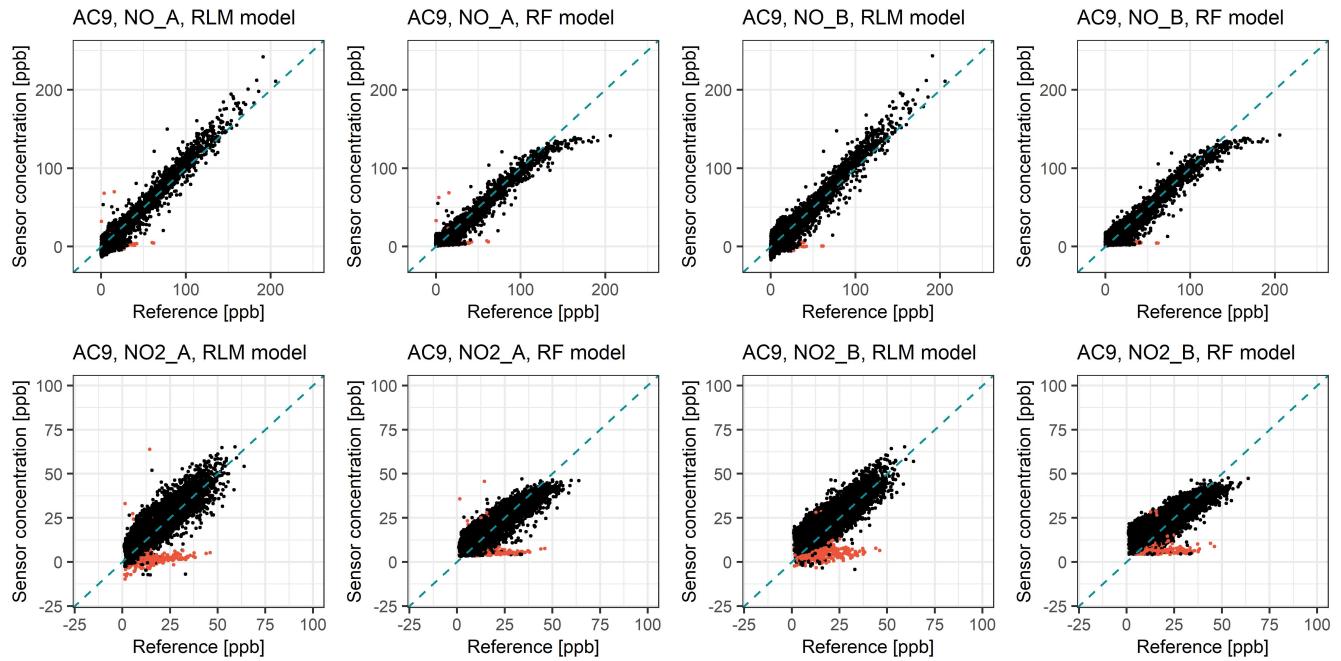
Figure S16. Filtered data points of AC009 during the second co-location period. Red-colored data points indicate the data which were eliminated by the sensor malfunction filtering process.
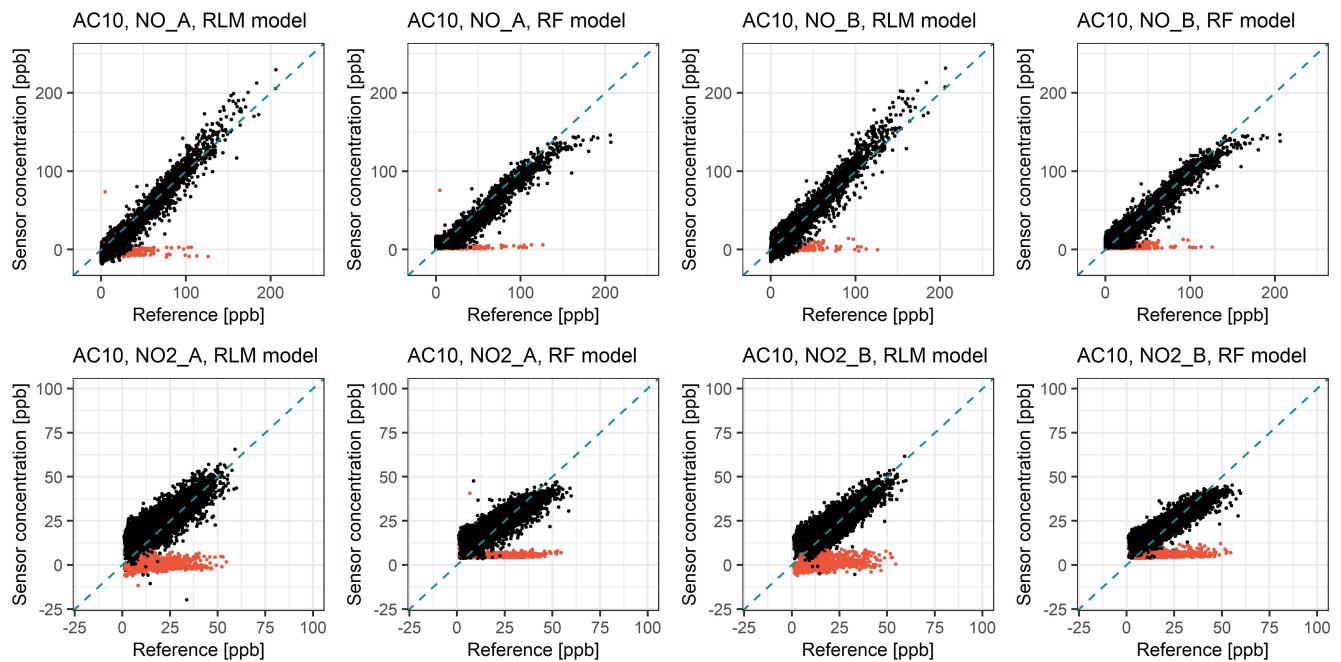
Figure S17. Filtered data points of AC010 during the second co-location period. Red-colored data points indicate the data which were eliminated by the sensor malfunction filtering process.
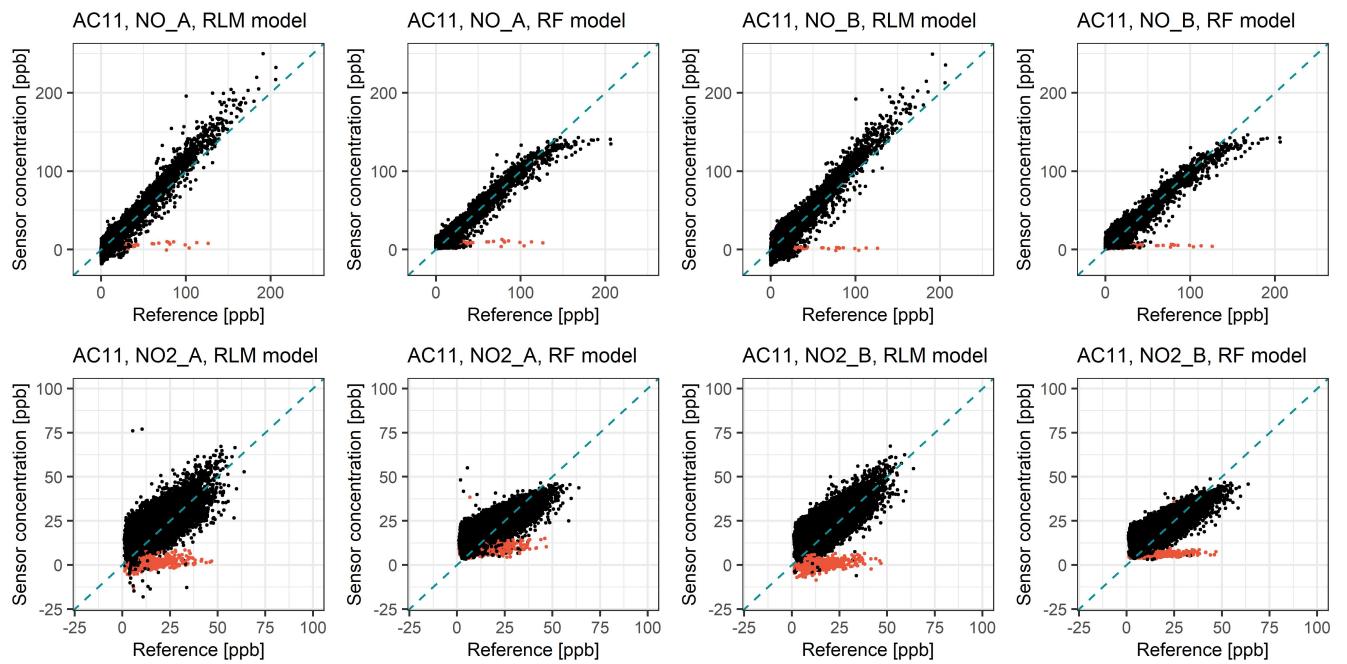
Figure S18. Filtered data points of AC011 during the second co-location period. Red-colored data points indicate the data which were eliminated by the sensor malfunction filtering process.
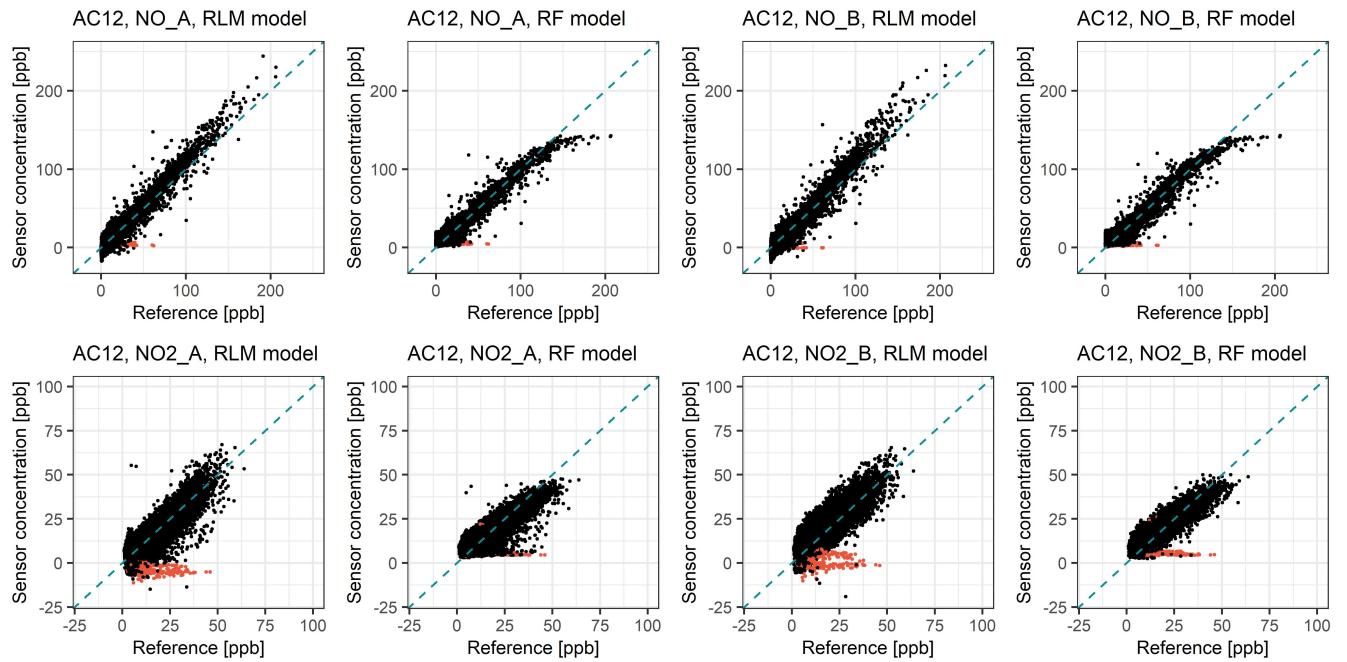
Figure S19. Filtered data points of AC012 during the second co-location period. Red-colored data points indicate the data which were eliminated by the sensor malfunction filtering process.